

## Fracture Behavior of Phosphorus-Doped Polycrystalline Fe-2.3%V Alloy

Pavel Lejček<sup>1,a</sup>, Jaroslav Pokluda<sup>2,b</sup>, Pavel Šandera<sup>2,c</sup>, Jana Horníková<sup>2,d</sup>,  
Bohumil Vlach<sup>2,e</sup> and Monika Jenko<sup>3,f</sup>

<sup>1</sup>Institute of Physics, AS CR, Na Slovance 2, 182 21 Praha 8, Czech Republic

<sup>2</sup>Brno University of Technology, Faculty of Mechanical Engineering., Institute of Engineering Physics, Technická 2, 616 69 Brno, Czech Republic

<sup>3</sup>Institute of Metals and Technology, Lepi pot 11, 1000 Ljubljana, Slovenia

<sup>a</sup>lejcekp@fzu.cz, <sup>b</sup>pokluda@fme.vutbr.cz, <sup>c</sup>sandera@fme.vutbr.cz, <sup>d</sup>hornikova@fme.vutbr.cz,  
<sup>e</sup>vlach@fme.vutbr.cz, <sup>f</sup>monika.jenko@imt.si

**Keywords:** Fe–P alloy, grain boundary segregation, intergranular fracture, impact test, Auger electron spectroscopy.

**Abstract.** Fracture behavior of a polycrystalline Fe–2.3%V alloy doped by 0.12% phosphorus is studied both experimentally and theoretically. Experiments show that the mode of the fracture depends on grain boundary segregation of phosphorus driven by annealing at different temperatures. The portion of the quasi-brittle fracture is related to measured grain boundary concentration of phosphorus. A comparison of theoretical simulations with experimental data has shown that intergranular fracture runs along grain boundaries containing more than about 17 at.% of segregated phosphorus. The mechanism and kinetics of fracture process could be also deduced.

### Introduction

Brittle fracture is one of the most dangerous failures occurring in metals and alloys. The brittleness of the material may be of intrinsic nature depending on temperature: there exists a critical temperature, so-called ductile-brittle transition temperature (DBTT), under which the material is brittle while it is ductile above it. Improper application of a material under this temperature can have catastrophic consequences, as was, for example, the sinking of the RMS Titanic nearly one hundred years ago. The material of Titanic – although representing the best-grade steel at that time – was characterized by coarse grain size and high level of inclusions so that DBTT was higher than +32°C. No wonder that this ship was catastrophically destroyed by brittle fracture during its impact with the iceberg at the water temperature of –2°C [1]... Besides intrinsic sources, the brittleness is often evoked by external effects, such as flawed material processing or segregation of deleterious impurities to grain boundaries. Grain boundary segregation results in a local enrichment of a thin but continuous interfacial layer throughout the polycrystalline material on the level of as much as several orders of magnitude higher comparing to the grain volume [2]. The most dangerous impurities segregating in bcc iron and steels are phosphorus, tin and antimony. For example, the disintegration of the rotor at Hinkley Point Power Station turbine generator in 1969 was caused by phosphorus segregation up to 50% at the grain boundaries of the 3Cr½Mo low-alloy steel containing few tenths percents of phosphorus in bulk [3].

To quantify the effect of impurity segregation to grain boundaries, we performed recently an extended study of fracture behavior and grain boundary chemistry in Fe–3%Si based alloy, which contained traces of phosphorus. Despite this study provided us with unambiguous results [4], the data may suffer by the fact that both silicon and phosphorus segregate at the grain boundaries and reduce the cohesion of the material [2]. Additionally, due to repulsive interaction between phosphorus and silicon a complex segregation behavior occurs (i.e. enrichment of phosphorus but

depletion by silicon) [5]. Much straightforward results in this respect should be obtained by measurement of phosphorus segregation and fracture behavior in phosphorus-doped iron or in an iron alloy containing an element, which is indifferent to phosphorus segregation. Because we planed to perform a thorough study in this field complemented by experiments on bicrystals, we did choose the phosphorus-doped Fe–2mass.%V base alloy. Here, the  $\gamma$ -phase is fully avoided and the system is bcc up to the congruent melting point so that it is possible to grow bicrystals from the melt. Vanadium does not affect the grain boundary cohesion significantly and, in addition, its segregation is expected to be rather low. From this point of view, we may consider this alloy as pseudobinary Fe–P system. In this work we refer on fracture behavior of polycrystalline Fe–2.3mass.%V base alloy with different level of phosphorus segregation at grain boundaries.

## Experimental

Polycrystals of an Fe–2.3 mass %V–0.12mass.%P alloy were prepared by hot rolling of the vacuum cast master alloy between 1370 K and 1070 K and annealing at 973 K for 1 hr so that an average grain size of 0.2 mm was achieved. The notched samples for fracture testing with dimensions of 50×7×5 mm were annealed for interfacial segregation at 1073 K for 24 h or at 973 K for 48 h or at 873 K for 72 h or at 773 K for 168 h.

Annealed samples were deformed in the three-point bending at room temperature using the testing machine Zwick Z 020. Because all conditions for  $K_{Ic}$  validity were not fulfilled, the fracture toughness  $K_{IJ}$  was evaluated according to ASTM E399–72 procedure. The data are listed in Table 1. It should be emphasized that the force-displacement curves of all specimens exhibited a short nonlinear part that indicated a rather short dislocation assisted stable crack growth before the fast unstable break. However, this initiation stage of such quasi-brittle fracture became negligible for prevailing portions of intergranular morphology on the fracture surface. Fracture surfaces of the samples were inspected by Philips XL-30 scanning electron microscope (SEM) and the portions of intergranular fracture,  $\eta$ , were determined and are also displayed in Table 1. The values correspond to the vicinity of the fatigue crack front, i.e. to the initiation stage of the quasi-brittle fracture process. As a rule, the  $\eta$ -values in the region of unstable fracture were found to be higher.

**Table 1** Statistical characteristics of experimental data on chemical composition of grain boundaries and on fracture behavior of polycrystalline Fe–2.3mass.%V–0.12mass.%P alloy.  $K_{IJ}$  ... fracture toughness,  $T$  ... annealing temperature,  $\eta$  ... portion of intergranular fracture,  $R_L$  and  $R_L^*$  ... linear (profile) roughness and  $R_L$  corrected to the portion of transcrystalline cleavage, respectively,  $k_{in,c}$  ...intrinsic fracture toughness ,  $X_P^\Phi$  and  $X_V^\Phi$  ... grain boundary concentrations of phosphorus and vanadium.

$T$ (K)	$\langle X_P^\Phi \rangle$ (at.%)	$\langle X_V^\Phi \rangle$ (at.%)	$\langle K_{IJ} \rangle$ (MPa.m <sup>1/2</sup> )	$\langle \eta \rangle$	$\langle R_L \rangle$	$\langle R_L^* \rangle$	$\langle k_{in,c} \rangle$ (MPa.m <sup>1/2</sup> )
773	25.3 ± 6.9	14.4 ± 9.2	24.5 ± 7.5	0.89 ± 0.07	3.6 ± 1.2	4.8 ± 2.2	7.9 ± 3.6
873	18.1 ± 8.9	9.2 ± 8.0	49.0 ± 9.4	0.47 ± 0.14	2.7 ± 0.8	4.6 ± 1.6	31.8 ± 10.3
973	19.4 ± 6.6	5.6 ± 5.6	66.4 ± 16.6	0.74 ± 0.07	4.6 ± 1.9	5.7 ± 2.2	28.8 ± 13.7
1073	20.6 ± 6.9	4.4 ± 2.0	38.8 ± 14.6	0.77 ± 0.03	4.7 ± 0.2	5.8 ± 0.1	14.6 ± 6.5

The composition of the grain boundaries was studied by Auger electron spectroscopy (AES) using Microlab 310F VG-Scientific facility equipped with a field emission gun. Notched cylindrical samples of the diameter of 5 mm and length of 30 mm were *in situ* impact fractured at about –120°C and subsequently analyzed in ultra high vacuum of  $5 \times 10^{-8}$  Pa. For analyses, a focussed

electron beam (approximately 10 nm in diameter) of the energy of 10 keV and of the current of 10 nA was used. To determine phosphorus and vanadium grain boundary concentrations, several tens AES analyses per sample were done at several intergranular facets. The Auger spectra were collected in the energy range 30–730 eV. The composition of the grain boundary monolayer was determined from the derivative Auger peak-to-peak heights measured at the fracture surface according to the standardless method [5] taking into account the attenuation length of Auger electrons and the backscattering term (Table 1).

## Results and discussion

AES measurement revealed that the annealing at different temperatures results in segregation of both phosphorus and vanadium (Table 1). The temperature dependence of their grain boundary concentrations is shown in Fig. 1. While the concentration of vanadium decreases with increasing temperature, phosphorus does not exhibit monotonous dependence showing minimum of segregation at 873 K followed by rather surprising increase with increasing temperature. This behavior clearly suggests that the segregation at lower temperatures is far of equilibrium. This is also proven by comparison of the results with the prediction of the grain boundary composition in Fe–P and Fe–V binary systems [6] (see the averaged experimental points and theoretical lines in Fig. 1). We suppose that only the data for 1073 K represent the equilibrium grain boundary composition. In all cases, the scatter of the data should predominantly reflect the anisotropy of grain boundary segregation.

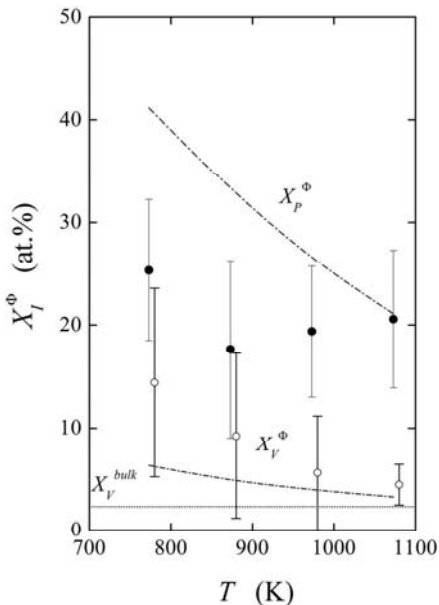


**Fig. 1** Concentrations  $X_T^\phi$  of phosphorus (solid circles) and vanadium (empty circles) at grain boundaries of polycrystalline Fe–2.3%V–0.12%P alloy at different temperatures. The dashed-dotted lines show predicted equilibrium concentrations of phosphorus and vanadium at general grain boundaries. The dotted line depicts vanadium bulk concentration.

Analysis of the fracture surfaces disclosed that the separation of the samples was predominantly of the intercrystalline nature accompanied by some amount of transcrystalline cleavage (Fig. 2). It should be noted that, with respect to a large mean grain size of 200  $\mu\text{m}$ , the transgranular cleavage

is observed here rather than the ductile dimple morphology typical for fine-grained polycrystalline iron.

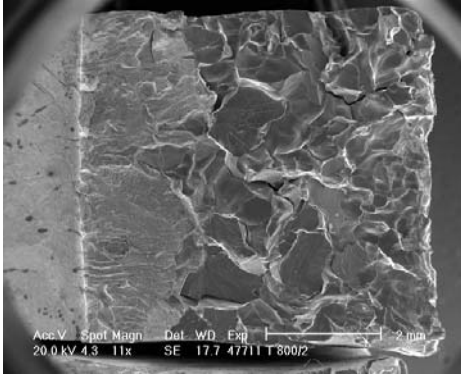


**Fig. 2** Fracture surface of polycrystalline Fe–2.3%V–0.12%P alloy annealed at 1073 K, broken at room temperature. Typical morphology of prevailing intercrystalline brittle fracture ( $\eta = 0.73$ ) with several transcrystalline cleavage facets near the fatigue pre-crack front is apparent in the middle of the fracture surface. On the left-hand site the notch and the pre-crack are clearly visible.

The surface ratio of the intercrystalline fracture morphology,  $\eta$ , changes with annealing temperature of the sample, i.e., with the level of interfacial segregation (Fig. 2). Let us construct the curves of the probability density vs. phosphorus concentration supposing the increment of the probability density to be  $1/N$  where  $N$  is the number of measured AES data at each temperature (Fig. 3). It is apparent that the experimental data are well correlated by the Gaussian cumulative distribution function  $F(x)$  for all four temperatures,

$$F(X_p^\Phi) = \int_{-\infty}^{X_p^\Phi} f(\xi) d\xi, \quad (1)$$

$$f(\xi) = \frac{1}{\sigma\sqrt{2\pi}} \exp\left[-\frac{1}{2}\left(\frac{\xi - \mu}{\sigma}\right)^2\right]$$

where  $f(\xi)$  is probability density function,  $\mu$  is the mean value and  $\sigma$  is the standard deviation.

The portion of the transcrystalline fracture should be proportional to  $F(X_p^\Phi)$  for some critical concentration of phosphorus,  $X_{Pc}$ . In other words, it is supposed that transcrystalline cleavage occurs when  $X_p^\Phi < X_{Pc}$  while for  $X_p^\Phi > X_{Pc}$  the intercrystalline fracture dominates. Portions of transcrystalline and intercrystalline fracture related to the critical value  $X_{Pc} = 17$  at.% (dashed lines) are marked in Fig. 3. The curves of probable portion of intergranular fracture for various selected  $X_{Pc}$  in the range of 5–20 at.% P, i.e. spline curves based on calculated points for individual annealing temperatures, are shown in Fig. 4, where they are also compared with the experimental values of  $\eta$ . It is apparent that the theoretical prediction for  $X_{Pc} = 17$  at.% P yields the best fit to averaged experimental data independently of annealing temperature. This means that all grain boundaries containing more than about 17 at. % of phosphorus fractured in an intergranular manner.

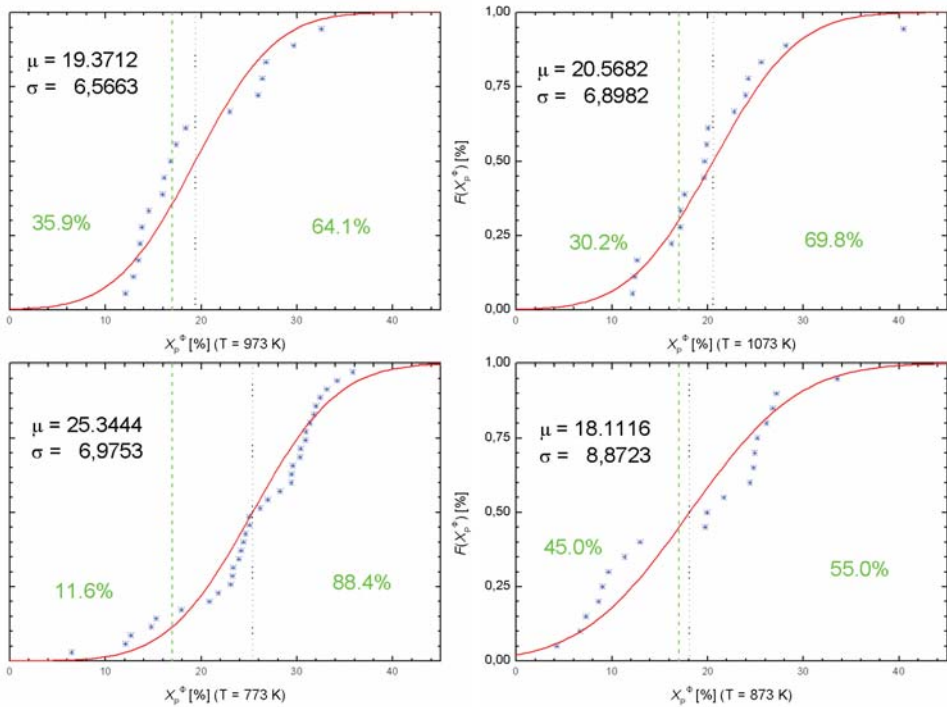


**Fig. 3** Distribution curves of the grain boundary concentration of phosphorus,  $X_p^\phi$ , at individual temperatures. Experimental points are correlated with Gaussian curves with characteristic parameters  $\mu$  and  $\sigma$ . Vertical dotted lines depict the medians. The portions of the transcrystalline (left) and intercrystalline (right) fracture corresponding to  $X_{Pc} = 17$  at.% (dashed lines) are also given.

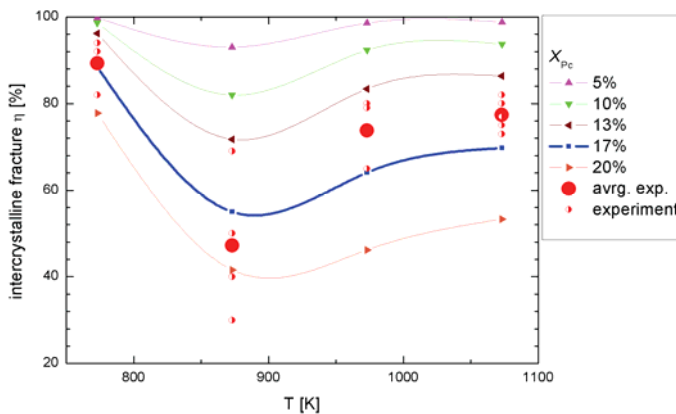


**Fig. 4** Comparison of calculated ratios of the intercrystalline fracture morphology for selected values of  $X_{Pc}$  (5 at.% to 20 at.%) with experimental data (semi-solid points). The averages of these values for individual temperatures are also shown (large solid points).

The presence of intergranularly fractured facets induces an extreme microscopical tortuosity of the crack front and, therefore, a strong geometrical (extrinsic) shielding of the crack tip occurs [7].

To obtain the values of both the intrinsic fracture toughness and the fracture energy at intercrystalline facets, the extrinsic effect has to be subtracted from the values of  $K_{II}$ . A 3D analysis of the profiles of the fracture surfaces was performed closely to the fatigue crack front that corresponds to the initiation of the intercrystalline fracture. The 3D reconstruction using the program code Mark III enabled us to evaluate the profile roughness  $R_L$ . An example of the tortuous profile is shown in Fig. 5. The coordinate  $z$  represents the height profile and the coordinate  $x$  runs along the crack front. The values of  $R_L$  were corrected to the ratio  $1-\eta$  of the transcrystalline morphology according to the relation  $R_L^* = (R_L - 1 + \eta)/\eta$ . Corrected values were used to determine the intrinsic fracture toughness,  $k_{int,c}$ , in frame of so-called general pyramidal model that enables the calculation of mean intrinsic values of the stress intensity factor  $k_{int}$  along the intergranular crack front:

$$k_{int}^2 = \frac{\pi - 2}{2\Theta_m (2R_L^* + \pi - 4)} \int_{-\Theta_m}^{\Theta_m} \left( k_1^2 + k_2^2 + \frac{k_3^2}{1 - \nu} \right) d\Theta, \quad (2)$$

where  $\Theta_m = \Phi$ ,  $R_L^* = (\cos\Phi)^{-1}$ ,  $\Phi$  is the deflection angle of the crack front in the pyramidal element and

$$\begin{aligned} k_1 &= \cos\left(\frac{\Theta}{2}\right) \left[ 2\nu \sin^2 \Phi + \cos^2\left(\frac{\Theta}{2}\right) \cos^2 \Phi \right], \\ k_2 &= \sin\left(\frac{\Theta}{2}\right) \cos^2\left(\frac{\Theta}{2}\right), \\ k_3 &= \cos\left(\frac{\Theta}{2}\right) \sin \Phi \cos \Phi \left[ 2\nu - \cos^2\left(\frac{\Theta}{2}\right) \right]. \end{aligned} \quad (3)$$

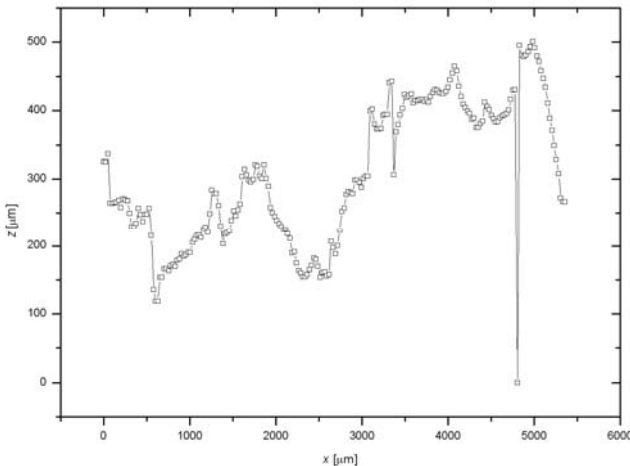


**Fig. 5** Profile of the tortuous crack front at initiation of an intercrystalline fracture.

Such calculated intrinsic fracture toughness  $k_{int,c}$  is plotted as a function of  $\eta$  in Fig. 6. An extrapolation of this dependence to 100% of intergranular fracture ( $\eta = 1$ ) enables us to obtain the

value of  $k_{int,c}$  that corresponds to a pure intergranular fracture. The data are significantly scattered as could be expected due to a pronounced anisotropy of phosphorus grain boundary segregation in the range of 1–35%. Despite this scatter, it is apparent that the dependence can be well linearly correlated and  $k_{int,c} \approx 3.8 \text{ MPa}\cdot\text{m}^{1/2}$ . This value well corresponds to the results of experimental as well as atomistic and discrete-dislocation simulations [8–10]. Molecular dynamics provides the initiation values of about  $1 \text{ MPa}\cdot\text{m}^{1/2}$  for cleavage in a perfect crystal of iron at 0 K. In these simulations, however, both the atomically sharp crack tip and the ideal configuration of crack/slip system are supposed. At room temperature, however, the dislocation emission accompanies the fatigue pre-crack growth and the crack front is blunted. This reduces the level of stress intensity range in comparison with an ideal crack and, consequently, the value extrapolated from the present experiments must be somewhat higher than that obtained from the theory.

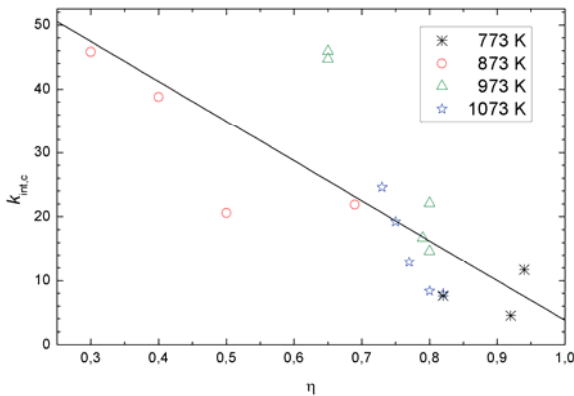


**Fig. 6** Plot of experimental values of fracture toughness,  $k_{int,c}$  vs. the ratio of the intercrystalline brittle fracture,  $\eta$ , for all annealing temperatures.

By considering  $k_{int,c} \approx 3.8 \text{ MPa}\cdot\text{m}^{1/2}$  in the relation

$$\gamma_{int,j} = \frac{k_{int,c}^2 (1-\nu)^2}{2E} \quad (4)$$

one obtains the mean value of the surface energy on intercrystalline facets,  $\gamma_i \approx 19 \text{ J}\cdot\text{m}^{-2}$ . This value is comparable with the surface energy of brittle cleavage in ferrite at very low temperatures. It is also in agreement with an estimate of  $20 \text{ J}\cdot\text{m}^{-2}$  found previously for an Fe–Si–P alloy [11]. We may conclude that more than 17 at.% of phosphorus causes a grain boundary embrittlement to this limit level. When applying  $\gamma_i \approx 19 \text{ J}\cdot\text{m}^{-2}$  to the classical Orowan relationship we nearly obtain the ideal tensile strength of a pure iron crystal. This result is not surprising taking into account the fact that *ab initio* calculations do not evidence direct effect of phosphorus on reduction of ideal bond strength in Fe–P base single crystals at 0 K [12].

The concentration of phosphorus at some grain boundaries along the crack front is well below the critical value of 17 at.%. The related grains fail by the dislocation-assisted transgranular cleavage fracture under intrinsic stress intensity factors as high as tens of  $\text{MPa}\cdot\text{m}^{1/2}$ . This is clearly seen from the extrapolation of experimental data in Fig. 6 to 100% of cleavage fracture ( $\eta = 0$ ). Such relatively high values are not only a consequence of the blunted tip of the fatigue pre-crack. The dislocation arrangements within the plastic zone both ahead the crack front and in the crack wake produce additional crack tip shielding [13]. In all our experimental samples, however, a competitive mechanism of low-energetic intergranular fracture has been enforced along supercritically segregated and suitably oriented grain boundaries already at  $k_{int,c}$ -values of the order

of  $\text{MPa}\cdot\text{m}^{1/2}$  just at the onset of the short crack initiation stage. In the vicinity of isolated geometrical ledges associated with such isolated intercrystalline facets, local peaks of the  $k$ -factor along the crack front were immediately induced. In this way, either the intergranular or the cleavage fracture could spread across the whole crack front. In dependence on the mean segregation level in a particular specimen, therefore, a mixed intergranular/transgranular fracture was produced near the fatigue pre-crack front during the short initiation stage. Thus, the subsequent unstable rupture could sometimes happen under intrinsic stress intensity factors much lower than tens of  $\text{MPa}\cdot\text{m}^{1/2}$ . During the following stage of a fast unstable fracture, the stress intensity factor rapidly increases and allows an immediate intergranular fracture along the whole crack front. This means that the portion of intergranular morphology increases with the distance from the fatigue pre-crack front. This is clearly seen in Fig. 2, where only a pure intergranular morphology appears near the right-hand site edge of the fracture surface that corresponds to a final stage of unstable crack propagation.

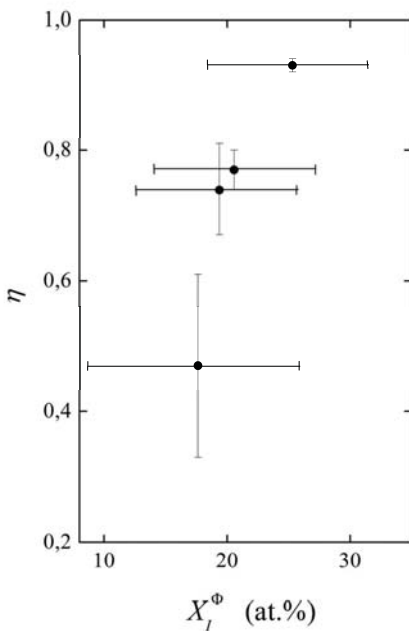


Fig. 7 Cumulative plot of experimental values of the ratio of the intercrystalline brittle fracture,  $\eta$ , vs. grain boundary concentration,  $X_I^\Phi$ , for all annealing temperatures.

Finally, let us comment the cumulative plot of  $\eta$  vs.  $X_I^\Phi$  (Fig. 7). It is unambiguously apparent that the ratio of the intercrystalline brittle fracture increases – although not necessarily linearly – with increasing grain boundary concentration of phosphorus. This fact suggests that the annealing temperature is not the decisive factor for the fracture behavior in case when the segregation is not allowed to reach equilibrium: the decisive factor for the amount of the intercrystalline fracture is the grain boundary concentration of phosphorus.

## Conclusions

Experimental and theoretical study of the fracture behavior of a polycrystalline Fe–2.3%V alloy doped by 0.12% phosphorus showed that there is a close relationship between the mode of the fracture and the segregation of phosphorus at the grain boundaries. It is shown that the critical phosphorus concentration for the predominant intercrystalline fracture is about 17 at.% and its portion increases with increasing phosphorus concentration at the grain boundaries. It is proven that temperature is not the decisive factor when the phosphorus segregation is far from equilibrium. The results enabled to evaluate basic characteristics of the fracture behavior of the alloy, which are close to those obtained by theoretical modeling. Moreover, the mechanism and kinetics of fracture process could be deduced.

## Acknowledgement

The authors are grateful to Czech Science Foundation for supporting the research under grants 106/05/0134 and 106/08/0369.

## References

- [1] K. Felkins, H.P. Leighly, Jr., and A. Jankovic, *J. Metals* 50 (1998), 12
- [2] E.D. Hondros, M.P. Seah, S. Hofmann and P. Lejček, in: *Physical Metallurgy*, edited by R.W. Cahn and P. Haasen, 4<sup>th</sup> edition, chapter 13, North-Holland, Amsterdam, NL (1996)
- [3] D. Kalderon, *Proc. Inst. Mech. Eng.* 186 (1972) 341
- [4] J. Janovec, M. Jenko, P. Lejček, J. Pokluda, *Mater. Sci. Eng. A* 462 (2007) 441
- [5] P. Lejček, *Anal. Chim. Acta* 297 (1994) 165
- [6] P. Lejček, S. Hofmann, J. Janovec, *Mater. Sci. Eng. A* 462 (2007) 76.
- [7] J. Pokluda, P. Šandera, J. Horníková, *Fat. Fract. Engng. Mater. Struct.* 27 (2004) 141.
- [8] R. Pippan, *Mater. Sci. Eng. A* 138 (1991) 1.
- [9] P. Hora *et al.*, *Engng. Fract. Mech.* (2008) in print.
- [10] F. Riemelmoser, *Int. J. Fract.* 85 (1997) 157.
- [11] J. Janovec, J. Pokluda, M. Jenko, P. Lejček, B. Vlach, J. Horníková, *Surf. Interface Anal.* 38 (2006) 401.
- [12] M. Černý, J. Pokluda, *Mater. Sci. Forum* 482 (2005) 135.
- [13] J. Pokluda, R. Pippan, *Mater. Sci. Eng. A* 462 (2007) 355.